

# A strange metal with a small Fermi surface and strong collective excitations

F.H.L. Essler<sup>1</sup> and A.M. Tsvelik<sup>2</sup>

<sup>1</sup> *Department of Physics, University of Oxford, 1 Keble Road, Oxford OX1 3NP, UK;*

<sup>2</sup> *Department of Physics, Brookhaven National Laboratory, Upton, NY 11973-5000, USA*

We develop a theory of a hybrid state, where quasi-particles coexist with strong collective modes, taking as a starting point a model of infinitely many one-dimensional Mott insulators weakly coupled by interchain tunneling. This state exists at an intermediate temperature range and undergoes an antiferromagnetic phase transition at temperatures much smaller than the Mott-Hubbard gap. The most peculiar feature of the hybrid state is that its Fermi surface volume is unrelated to the electron density. We present a self-consistent derivation of the low energy effective action for our model.

PACS numbers: 71.10.Pm, 72.80.Sk

## I. INTRODUCTION

The presence of strong collective modes interacting with quasi-particles is a distinctive feature of many strongly interacting systems such as 'bad' metals, weakly doped Mott insulators (such as the cuprates) and heavy fermion materials. This interaction is believed to result in a variety of unusual phenomena observed in these systems such as the violation of the Mott-Regel limit in the temperature dependence of the electrical resistivity of bad metals or the absence of quasi-particle peaks in the spectral function of the cuprates. The lack of non-perturbative techniques in dimensions higher than one makes a detailed theoretical description of these phenomena quite challenging. One successful approach has been developed by Chubukov, Schmalian and Abanov, who have studied the so-called spin-fermion model put forward by D. Pines<sup>1</sup>. This model is semi-phenomenological and postulates the existence of a strong, coherent, collective mode, which interacts with quasi-particles located in the vicinity of a Fermi surface. This model is reviewed comprehensively in Refs [2] and has proven quite successful in explaining various properties of the cuprates. However, a derivation from a microscopic Hamiltonian is lacking.

In this paper we provide a microscopic derivation of a model in the same class as the spin-fermion model of Pines and Chubukov. Namely, we continue to develop a theory of a hybrid state combining features of a Landau Fermi liquid and a Mott insulator suggested in Ref.[3]. This state is characterized by the coexistence of well-developed collective modes with quasi-particles. The latter ones have a small Fermi surface (SFS), the volume of which is unrelated to the total number of electrons. By definition, the Fermi surface (FS) is small if its volume is less than the maximum volume allowed by Luttinger's theorem<sup>4,5,6,7</sup>. The existence of such a state does not contradict Luttinger's theorem since the latter, contrary to popular belief, does not fix the volume of FS. Instead the theorem states that the electron density  $n$  is proportional to the volume of phase space enclosed by the surface where the single electron Green's function changes

its sign

$$n = \frac{2}{(2\pi)^d} \int_{G(\omega=0, \mathbf{k}) > 0} d^d k. \quad (1)$$

When the Green's function has zeroes, the Fermi surface constitutes only a part of this surface, namely the one where  $G(0, \mathbf{k}) \rightarrow \infty$ . Hence Luttinger's theorem (1) does not even require the existence of a Fermi surface: the Green's function may only have zeroes and no poles, as it is the case for superconductors<sup>5</sup> and certain one-dimensional systems, in which the spectral gap is generated dynamically (for the latter case a general proof is outlined in Ref. [8]).

A metallic state with a small FS would necessarily be associated with a Green's function that has both poles and zeroes at  $\omega = 0$ . In our previous work [3] we suggested a model for such a state based on the quasi-one-dimensional Hubbard model at half filling. The transverse hopping was treated in a Random Phase approximation (RPA). In order to understand the conditions of stability of such an exotic metal, one has to go beyond RPA, which is the main subject of the present paper. Experimental indications of the existence of SFS states come from ARPES measurements in underdoped cuprates<sup>9</sup> and from the Hall effect measurements in heavy fermion materials<sup>10</sup>.

Before turning to the calculations, we shall give a qualitative account of the physics we are after. Our starting point is an *ensemble of uncoupled, Mott insulating chains*. The relevant energy scale is the 1D Mott gap  $m$ . We consider finite temperatures  $T$  such that  $T \ll m$ . The physics is purely one dimensional.

We then turn on a small *long range interchain tunneling* with characteristic energy scale  $t_\perp$ . Clearly, at zero temperature the hopping between chains will be essential and induce a 3D ordered state. On the other hand, in the window

$$t_\perp \ll T, \tilde{t}_\perp(\mathbf{k}) \ll m, \quad (2)$$

we will recover the physics of 1D Mott insulating chains. Here  $\tilde{t}_\perp(\mathbf{k})$  denotes the Fourier transform of the interchain tunneling. Furthermore, as  $T \ll m$  we may to a

good approximation work with zero temperature quantities in many instances.

The crucial point is that while  $t_\perp$  remains much smaller than the Mott gap  $m$ , the Fourier transform  $\tilde{t}_\perp(\mathbf{k})$  can become comparable to  $m$  in some region of the Brillouin zone, i.e. we may have a situation where

$$t_\perp \ll T \ll \tilde{t}(\mathbf{0}) \approx m. \quad (3)$$

In this case an interesting “hybrid” state combining 1D with 3D features develops. In particular, the low energy sector corresponds to a 3D metal with a small Fermi surface and quasi-particles interacting with well-developed collective modes. The existence of the regime (3) is ensured by making the interchain tunneling long ranged.

The dimensional crossover from a quasi one dimensional Mott insulator to an anisotropic 3D Fermi liquid as a function of the strength  $t_\perp$  of the interchain hopping is sketched in Fig. 1.

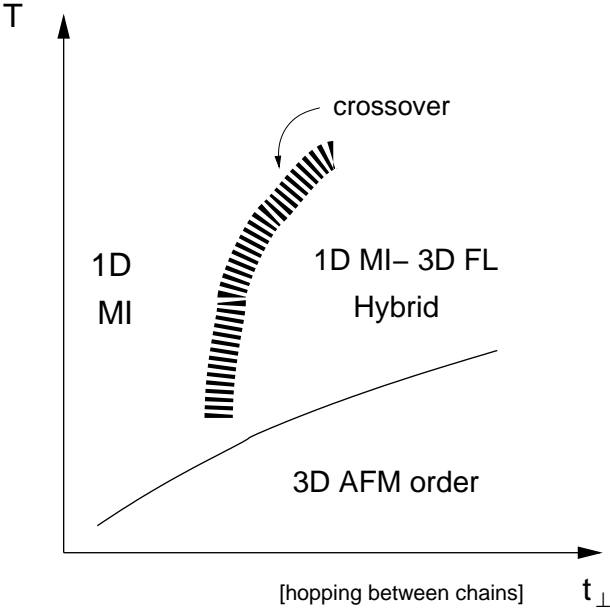


FIG. 1: Cartoon Phase Diagram for  $T \ll m$  for weakly coupled 1D Mott insulators, where  $m$  is the 1D Mott gap.

The purpose of the present work is to derive an effective theory for the low-energy degrees of freedom in the “1D Mott insulator/3D Fermi liquid hybrid” regime and to analyze its instabilities towards 3D order at sufficiently low temperatures.

## II. THE MODEL

The model we study is the Hubbard model with a strongly anisotropic hopping:

$$H = -t \sum_{n,\mathbf{l},\sigma} \left[ c_{n,\mathbf{l},\sigma}^\dagger c_{n+1,\mathbf{l},\sigma} + \text{h.c.} \right] + U \sum_{n,\mathbf{l}} n_{j,\mathbf{l},\uparrow} n_{j,\mathbf{l},\downarrow} + \sum_{\mathbf{l},\mathbf{m},n,p,\sigma} t_{\mathbf{l}\mathbf{m}}^{np} c_{n,\mathbf{l},\sigma}^\dagger c_{p,\mathbf{m},\sigma}. \quad (4)$$

For definiteness we consider the chain direction to be  $z$ , so that  $\mathbf{l} = (l_x, l_y)$ ,  $\mathbf{m} = (m_x, m_y)$  label Hubbard chains and  $n, p$  label the sites along a given chain.

As we have mentioned before, the hopping integrals in the transverse directions are supposed to be small in comparison to  $t$ . In the limit  $t_\perp = 0$  and at half filling the model has a Mott-Hubbard gap  $m$ . We work in a regime where the magnitude of this gap is much smaller than the bandwidth  $W \approx 4t$ . In our previous paper<sup>3</sup> the transverse hopping was treated in a Random Phase approximation (RPA). In order to suppress corrections to RPA (at least in some temperature interval) we assume that the transverse hopping is long ranged (see below).

### A. Uncoupled, Mott insulating chains

Let us briefly discuss the low-energy physics for uncoupled chains. In order to ease notations we suppress the chain index ( $\mathbf{l}$ ). Keeping only low-energy modes around the two Fermi points  $\pm k_F$ , the electron annihilation operators are decomposed as

$$c_{n,\sigma} = \sqrt{a_0} [\exp(ik_F x) R_\sigma(x) + \exp(-ik_F x) L_\sigma(x)], \quad (5)$$

where  $a_0$  is the lattice spacing,  $x = ja_0$  and  $k_F = \pi/2a_0$ . The fermionic creation operators for left and right moving Fermions are bosonized, using the following conventions

$$L_\sigma^\dagger(x) = \frac{\eta_\sigma}{\sqrt{2\pi}} e^{if_\sigma \pi/4} \exp\left(-\frac{i}{2}\bar{\phi}_c\right) \exp\left(-\frac{if_\sigma}{2}\bar{\phi}_s\right), \\ R_\sigma^\dagger(x) = \frac{\eta_\sigma}{\sqrt{2\pi}} e^{if_\sigma \pi/4} \exp\left(\frac{i}{2}\phi_c\right) \exp\left(\frac{if_\sigma}{2}\phi_s\right), \quad (6)$$

where  $\eta_a$  are Klein factors with  $\{\eta_a, \eta_b\} = 2\delta_{ab}$  and where  $f_\uparrow = 1$ ,  $f_\downarrow = -1$ . The chiral boson fields  $\phi_a$  and  $\bar{\phi}_a$  fulfil the following commutation relations

$$[\phi_a(x), \bar{\phi}_a(y)] = 2\pi i, \quad a = c, s. \quad (7)$$

In terms of the chiral fields  $\phi_a$  and  $\bar{\phi}_a$  we define canonical Bose fields  $\Phi_a$  and their dual fields  $\Theta_a$  by

$$\Phi_a = \phi_a + \bar{\phi}_a, \quad \Theta_a = \phi_a - \bar{\phi}_a. \quad (8)$$

The low-energy effective Hamiltonian density for a single chain takes the following bosonic form

$$\mathcal{H}_s = \frac{v_s}{16\pi} [(\partial_x \Theta_s)^2 + (\partial_x \Phi_s)^2] - g \mathbf{J} \cdot \bar{\mathbf{J}}, \\ \mathcal{H}_c = \frac{v_c}{16\pi} [(\partial_x \Theta_c)^2 + (\partial_x \Phi_c)^2] + g \mathbf{I} \cdot \bar{\mathbf{I}}. \quad (9)$$

Here  $I^\alpha$  and  $\bar{I}^\alpha$  ( $J^\alpha$  and  $\bar{J}^\alpha$ ) are the chiral components of the  $SU(2)$  pseudospin (spin) currents

$$\begin{aligned} I^z &= -\frac{1}{4\pi} \partial_x \phi_c, & I^+ &= \frac{\eta_\uparrow \eta_\downarrow}{2\pi} e^{i\phi_c}, \\ J^z &= -\frac{1}{4\pi} \partial_x \phi_s, & J^+ &= i \frac{\eta_\uparrow \eta_\downarrow}{2\pi} e^{i\phi_s}. \end{aligned} \quad (10)$$

The current-current interaction in the spin sector of (9) is marginally irrelevant and we will ignore it in what follows. We note that doing so enhances the symmetry in the spin sector from  $SU(2)$  (spin rotational symmetry) to  $SU(2) \times SU(2)$  (rotational symmetry of the left and right sectors).

### 1. Single-Particle Green's Function

The single-particle Green's function for the half-filled Hubbard model was obtained in the framework of the formfactor approach in Refs [3,14]. In particular, when the charge and spin velocities are equal we have

$$G_0(\omega, \pm k_F + q) = \frac{Z_0}{i\omega \mp vq} \left[ 1 - \frac{m}{\sqrt{m^2 + \omega^2 + (vq)^2}} \right], \quad (11)$$

where  $Z_0 \approx 0.921862$ . In order to obtain the above expression for  $G_0$  we took into account only processes involving the emission of a single massive holon and a cascade of gapless spinons.

### 2. Spin Sector

The spin operators  $S_n^\alpha = \frac{1}{2} c_{n,a}^\dagger \sigma_{ab}^\alpha c_{n,b}$  are expressed in terms of the left and right moving Fermi fields by

$$\begin{aligned} S_j^\alpha &\simeq (-1)^j \frac{a_0}{2} [R_a^\dagger(x) \sigma_{ab}^\alpha L_b(x) + \text{h.c.}] \\ &\quad + \frac{a_0}{2} [R_a^\dagger(x) \sigma_{ab}^\alpha R_b(x) + R \rightarrow L] \\ &\equiv a_0 [(-1)^j n^\alpha(x) + J^\alpha(x)]. \end{aligned} \quad (12)$$

The bosonized expressions for the staggered components of the spin operators are

$$R_a^\dagger(x) \sigma_{ab}^\alpha L_b(x) \simeq \frac{1}{\pi i \sqrt{2a_0}} \exp\left(\frac{i}{2} \Phi_c\right) \text{tr}(g\sigma^\alpha), \quad (13)$$

where we have replaced the product of Klein factors by their expectation value

$$\langle \eta_\uparrow \eta_\downarrow \rangle = -i, \quad (14)$$

and where the matrix field  $g$  is expressed in terms of the spin boson  $\Phi_s$  and its dual field  $\Theta_s$  by

$$g = \sqrt{\frac{a_0}{2}} \begin{pmatrix} \exp\left(\frac{i}{2} \Phi_s\right) & i \exp\left(-\frac{i}{2} \Theta_s\right) \\ i \exp\left(\frac{i}{2} \Theta_s\right) & \exp\left(-\frac{i}{2} \Phi_s\right) \end{pmatrix}. \quad (15)$$

At  $T = 0$  we have

$$\langle g_{\alpha\beta}(\tau, x) g_{\gamma\delta}^\dagger(0, 0) \rangle = \delta_{\alpha\delta} \delta_{\beta\gamma} \frac{a_0}{2\sqrt{v^2 \tau^2 + x^2}}. \quad (16)$$

Using (15) one can easily calculate multi-point correlation functions of  $g$ .

The action (9) describing the collective spin excitations on each chain is equivalent to the  $SU_1(2)$  Wess-Zumino-Novikov-Witten (WZNW) model once we drop the marginally irrelevant interaction of spin currents. The WZNW action for the matrix field  $g(\tau, x)$  is given by

$$\begin{aligned} W[g] &= \frac{1}{16\pi} \int d^2x \text{Tr} [\partial^\mu g^\dagger \partial_\mu g] \\ &\quad + \frac{\epsilon_{\mu\nu\lambda}}{24\pi} \int_B d^3x \text{Tr} [g^\dagger \partial^\mu g g^\dagger \partial^\nu g g^\dagger \partial^\lambda g], \end{aligned} \quad (17)$$

where  $x_1 = v\tau$ ,  $x_2 = x$ ,  $\partial_\mu = \frac{\partial}{\partial x^\mu}$ ,  $B$  is a three dimensional half-space ( $x_3 \leq 0$ ) whose boundary at  $x_3 = 0$  coincides with the two-dimensional  $(v\tau, x)$ -plane and  $g$  is an arbitrary extrapolation of the function defined on the two-dimensional space  $x_3 = 0$ , which approaches 1 at  $x_3 \rightarrow -\infty$ . The action (17) is invariant under  $SU(2) \times SU(2)$  transformations  $g \rightarrow Ug\tilde{U}^\dagger$ . The marginally irrelevant interactions of spin currents breaks this symmetry down to the diagonal spin-rotational  $SU(2)$   $g \rightarrow UgU^\dagger$ . The form (17) of the action for the spin degrees of freedom is significantly more complicated than the free boson representation (9). The latter is very convenient for calculations in one dimension, but may be less useful when one considers interchain coupling due to the fact that the dual field  $\Theta_s$  is non-local with respect to  $\Phi_s$ . The formulation in terms of the matrix field  $g$  has the advantage of the fundamental field being the order parameter itself. In fact,  $W[g]$  is the Ginzburg-Landau action for a 1D spin-1/2 antiferromagnet.

### 3. Three Point Function

An important ingredient in our analysis are three-point functions of the form  $\langle \text{Tr}[g(\mathbf{z})\sigma^\alpha] R_a^\dagger(\mathbf{z}_1) L_b(\mathbf{z}_2) \rangle$ . The large-distance asymptotics of these correlators can be evaluated by using the results of [14]

$$\begin{aligned}
\langle \text{Tr}[g(\mathbf{z})\sigma^+] R_{\downarrow}^{\dagger}(\mathbf{z}_1) L_{\uparrow}(\mathbf{z}_2) \rangle &= -i \frac{\langle \eta_{\downarrow} \eta_{\uparrow} \rangle}{2\pi} \langle \text{Tr}[g(\mathbf{z})\sigma^+] e^{-\frac{i}{2}\phi_s(\mathbf{z}_1)} e^{\frac{i}{2}\bar{\phi}_s(\mathbf{z}_2)} \rangle_s \langle e^{\frac{i}{2}\phi_c(\mathbf{z}_1)} e^{\frac{i}{2}\bar{\phi}_c(\mathbf{z}_2)} \rangle_c \\
&\simeq i \frac{\langle \eta_{\downarrow} \eta_{\uparrow} \rangle}{2\pi} \langle \text{Tr}[g(\mathbf{z})\sigma^+] e^{-\frac{i}{2}\phi_s(\mathbf{z}_1)} e^{\frac{i}{2}\bar{\phi}_s(\mathbf{z}_2)} \rangle_s \frac{Z_1 \sqrt{a_0}}{\pi} e^{\frac{3i\pi}{4}} K_0(mr_{12}) \\
&\simeq \hat{Z} \langle \eta_{\downarrow} \eta_{\uparrow} \rangle K_0(mr_{12}) \langle \text{Tr}[g(\mathbf{z})\sigma^+] \text{Tr}[g(\mathbf{z}_+)\sigma^-] \rangle_s,
\end{aligned} \tag{18}$$

where  $\mathbf{z}_{1,2} = (\tau_{1,2}, x_{1,2})$ ,  $r_{12} = |\mathbf{z}_1 - \mathbf{z}_2|$  and  $\mathbf{z}_+ = (\frac{\tau_1 + \tau_2}{2}, \frac{x_1 + x_2}{2})$ . The constant  $\hat{Z}$  is related to the normalisation  $Z_0$  of the single-particle Green's function by<sup>14</sup>

$$\hat{Z} = -\frac{Z_0}{\pi^{\frac{3}{2}}} \sqrt{\frac{m}{va_0}}. \tag{19}$$

The calculation we have just carried out can be summarized by the following approximate relations

$$\begin{aligned}
R_a^{\dagger}(\mathbf{z}_1) \sigma_{ab}^{\alpha} L_b(\mathbf{z}_2) &\longrightarrow i \hat{Z} K_0(mr_{12}) \text{Tr}[g(\mathbf{z}_+)\sigma^{\alpha}], \\
L_a^{\dagger}(\mathbf{z}_1) \sigma_{ab}^{\alpha} R_b(\mathbf{z}_2) &\longrightarrow i \hat{Z} K_0(mr_{12}) \text{Tr}[g(\mathbf{z}_+)\sigma^{\alpha}].
\end{aligned} \tag{20}$$

The approximation (20) fails at small distances. In order to remove the logarithmic singularity of  $K_0$  one needs to include terms corresponding to the multiple production of solitons and antisolitons. At energies much smaller than the Mott gap, the fusion (20) gives rise to the spin-fermion vertex depicted on Fig. 2.



FIG. 2: The fermion-spinon interaction generated by fusion (20).

## B. Long range interchain hopping

In order to have a small parameter in our theory we consider the interchain hopping to be long-ranged, such that the Fourier transform of the hopping matrix elements strongly depends on the wave vector. This is a well-known trick (see, for example Ref. [15]) and results in a controlled “loop” expansion, where every integration over the transverse momenta leads to a small factor  $\kappa_0^2$  in three dimensions, where  $\kappa_0$  is the inverse range of the interchain tunnelling. The interchain hopping may be taken long ranged both along and perpendicular to the chain direction. In order to simplify the calculations, we will constrain our discussion to the case where  $t_{\mathbf{lm}}^{np} = t(\mathbf{l} - \mathbf{m})\delta_{n,p}$ , i.e. the interchain hopping has no component along the chain direction and depends only on the distance between chains. The Fourier transform

of the interchain tunneling is then given by

$$\tilde{t}_{\perp}(\mathbf{k}_{\perp}) = \sum_{\mathbf{m}} t_{\mathbf{l}\mathbf{m}} \exp(i\mathbf{k}_{\perp} \cdot (\mathbf{l} - \mathbf{m})a_{\perp}). \tag{21}$$

In the following we choose the interchain hopping such that it respects the particle-hole symmetry

$$c_{n,\mathbf{l},\sigma} \longleftrightarrow (-1)^{n+l_x+l_y} c_{n,\mathbf{l},\sigma}^{\dagger}, \tag{22}$$

which implies that

$$\tilde{t}_{\perp}(\mathbf{k}_{\perp} + \mathbf{Q}) = -\tilde{t}_{\perp}(\mathbf{k}_{\perp}), \tag{23}$$

where

$$\mathbf{Q} = \left( \frac{\pi}{a_{\perp}}, \frac{\pi}{a_{\perp}} \right) \tag{24}$$

is the antiferromagnetic wave vector in the direction transverse to the chains. It is straightforward to generalize our following analysis to non particle-hole symmetric cases. The basic assumptions underlying our model are then summarized in the following inequalities:

$$W \gg m \sim |\tilde{t}_{\perp}(\mathbf{0})| = |\tilde{t}_{\perp}(\mathbf{Q})| \gg \tilde{t}_{\perp}(\mathbf{p}_{\perp}). \tag{25}$$

Here  $W = 4t$  and  $m$  are the band width and Mott gap for uncoupled chains respectively and  $|\mathbf{p}_{\perp}a_{\perp}|, |(\mathbf{p}_{\perp} - \mathbf{Q})a_{\perp}| \gg \kappa_0$ . The small parameter  $\kappa_0$  characterizes the support of  $\tilde{t}_{\perp}(\mathbf{k}_{\perp})$  in momentum space. The precise form of the momentum dependence of  $\tilde{t}_{\perp}$  is supposedly unimportant, but in order to simplify the concrete calculations we shall use the following model:

$$\tilde{t}_{\perp}(\mathbf{k}_{\perp}) = -\frac{t_0}{1 + |\mathbf{k}_{\perp}a_{\perp}|^2\kappa_0^{-2}}, \quad |\mathbf{k}_{\perp}a_{\perp}| \ll 1. \tag{26}$$

Within the model (26) the integration over the transverse wave vectors may be replaced by integration over  $t \equiv t_{\perp}(\mathbf{k}_{\perp})$

$$a_{\perp}^2 \int \frac{d^2 k_{\perp}}{4\pi^2} f(t) \approx \frac{\kappa_0^2 t_0}{4\pi} \int_{\frac{\kappa_0^2 t_0}{4\pi^2}}^{t_0} \frac{dt}{t^2} [f(t) + f(-t)]. \tag{27}$$

Some readers may find that our approach is similar to Dynamical Mean Field theory in an *infinitely dimensional*

space. This is not the case: the difference comes from the fact that in our model the transverse density of states is constant on the zone boundary. This feature strengthens the influence of fermionic coherent modes and utterly changes the physics (see the discussion in the Conclusions).

### III. PERTURBATION THEORY IN THE INTERCHAIN TUNNELING

As we have already mentioned, the perturbation theory in the interchain tunneling can be reorganized in terms of a loop expansion. Every integration over the transverse momenta generates a small factor  $\kappa_0^2$ . We will refer to the leading order  $\mathcal{O}(\kappa_0^0)$  in this expansion as “Random Phase Approximation” (RPA).

The RPA expression for the single particle Green’s function  $G$  was derived in Ref. [3] and is given by

$$G(\omega, \pm k_F + q, \mathbf{k}_\perp) = \frac{G_0(\omega, \pm k_F + q)}{1 - \tilde{t}_\perp(\mathbf{k}_\perp) G_0(\omega, \pm k_F + q)}. \quad (28)$$

Here  $G_0$  is the single-particle Green’s function for an individual chain (11). In a purely one-dimensional Mott insulator the electron is a composite particle and as a result the spectral function is incoherent. Coherent electronic excitations reappear as soon as the interchain tunneling is turned on. They can be understood as antiholon-spinon bound states and occur at energies *below* the Mott gap. When  $t_\perp$  exceeds a certain critical value, the dispersion of the coherent mode crosses the chemical potential and a Fermi surface is formed. As a consequence of particle-hole symmetry, at half-filling this Fermi surface consists of electron- and hole-like pockets of equal volume. A sketch of such a Fermi surface is shown in Fig. 3. A convenient measure for the strength of the interchain coupling is given by the quantity

$$\mathcal{Z} \equiv \frac{Z_0 t_0}{m}, \quad (29)$$

where  $t_0$  is defined in (26). The RPA form (28) for the Green’s function features a pole corresponding to a coherent quasi-particle mode. This mode crosses the chemical potential when  $\mathcal{Z}$  exceeds the critical value

$$\mathcal{Z}_c = 3.33019 \dots, \quad (30)$$

and a Fermi surface is present for all  $\mathcal{Z} > \mathcal{Z}_c$ .

Having in hand the expression for the chain single-particle Green’s function, we may use it to define a dressed interchain hopping  $\tilde{T}_{R,L}(\omega, q, \mathbf{k}_\perp)$  by summing the diagrams shown in Fig. 4. This results in

$$T_{R,L}(\omega, q, \mathbf{k}_\perp) = \frac{\tilde{t}_\perp(\mathbf{k}_\perp)}{1 - \tilde{t}(\mathbf{k}_\perp) G_0(\omega, \pm k_F + q)}, \quad (31)$$

where the  $+$  sign corresponds to  $R$  and the  $-$  sign to  $L$  respectively. We note that the dressed interchain hopping is equal to the propagator of the Hubbard-Stratonovich field that can be introduced to decouple the interchain hopping<sup>11</sup>.

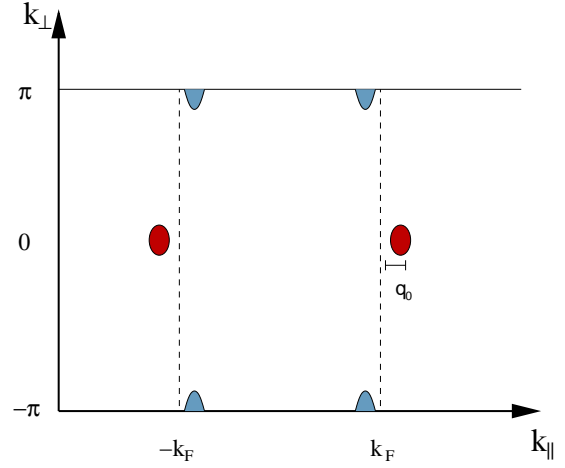


FIG. 3: The Brillouin zone with the electron (red ovals) and hole-like (blue semi-ovals) Fermi pockets of a two-dimensional lattice. The noninteracting Fermi surface is shown as a dashed line.

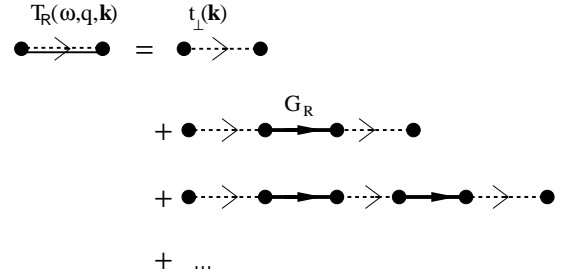


FIG. 4: The dressed interchain hopping.

#### A. The Spin Sector in RPA

In the RPA, the spin sector remains one-dimensional and critical. This can be seen as follows. Let us consider the real-space correlator between the staggered components of spins on different chains  $\mathbf{l}$  and  $\mathbf{m}$

$$\langle n_{j,\mathbf{l}}^+(t) n_{\mathbf{l},\mathbf{m}}^-(0) \rangle. \quad (32)$$

Within perturbation theory in the interchain hopping, we need at least one right moving and left moving fermion operator each on chains  $\mathbf{l}$  and  $\mathbf{m}$  in order to obtain a nonzero expectation value in the spin sector. The only ways to achieve this are shown in Fig. 5. Here the dashed lines denote the bare interchain hopping, ellipses enclosing two black (white) circles represent the purely 1D Green’s function of right (left) moving electrons on a given chain and the ellipses enclosing two circles and a hexagon stand for the three-point function (18). Clearly all such diagrams involve at least one integration over the transverse momentum. Hence, within the RPA spin-spin correlation functions remain entirely

one-dimensional and spins on different chains remain uncorrelated.

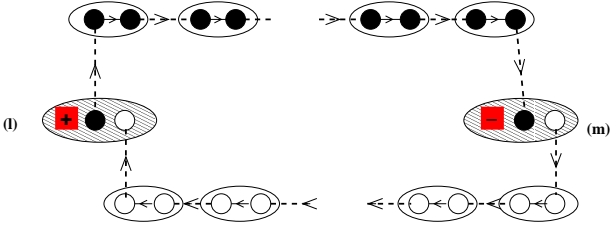


FIG. 5: Real-space diagrams that contribute to the two-point function of staggered magnetizations between chains (l) and (m).

### B. Excitation Spectrum in RPA

From the discussion above it is clear that for sufficiently strong interchain hopping  $\mathcal{Z} > \mathcal{Z}_c$  the RPA leads to two types of gapless excitations

- Fermionic particle and hole excitations over the Fermi surface with anisotropic 3D dispersions.
- Collective excitations of the spin degrees of freedom. These are of a purely 1D nature and do not have a dispersion in the direction transverse to the chains.

If one goes beyond the RPA, interactions between these two types of excitations will be generated. In the following we determine the form of these interactions and study their effects. To go beyond the RPA in principle requires the knowledge of the two-particle Green's function of uncoupled Mott-insulating chains. However, if one restricts one's attention to the regime of energies small compared to the Mott gap, the three-point function  $\hat{3}$ point (which corresponds to a particular limit of the two-particle Green's function) suffices.

## IV. INTERCHAIN EXCHANGE AND ESTIMATE OF THE TRANSITION TEMPERATURE

Although it is obvious that corrections to RPA are of higher order in the small parameter  $\kappa_0$ , they will di-

verge at small temperatures. Therefore RPA works only at finite temperatures and for its consistency the transition temperature (below which the system is three-dimensionally ordered) must be much smaller than the Mott-Hubbard gap  $m$ . It is therefore important to estimate the corresponding corrections to RPA and their temperature dependence. As the first step in taking into account corrections to RPA we have to estimate the interchain RKKY interaction. As we have shown in section  $\hat{3}$ -point, there is a three-point “vertex” that couples the spin degrees of freedom to the fermionic quasi-particles. In second order perturbation theory in this interaction, an interchain exchange interaction between the spin degrees of freedom is generated. The corresponding action is given by

$$S_{xc} = \int \prod_{j=1}^2 d\tau_j dx_j \sum_{\mathbf{l} \neq \mathbf{m}} J_{\mathbf{l}\mathbf{m}}(x_1 - x_2, \tau_1 - \tau_2) \times \text{Tr} [g_{\mathbf{l}}(\tau_1, x_1) g_{\mathbf{m}}^\dagger(\tau_2, x_2)] . \quad (33)$$

The Fourier transform of the leading order (in  $\kappa_0$ ) exchange matrix element is given by the “bubble” diagram shown in Fig. 6, where the double lines are the dressed interchain hoppings for left and right moving fermions and the squares denote the elements of the matrix field. The result is

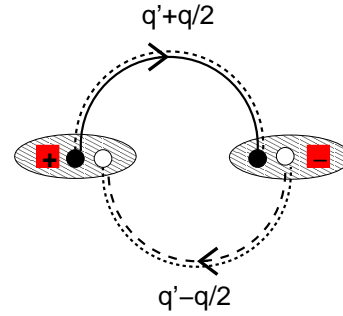


FIG. 6: Leading order  $\mathcal{O}(\kappa_0^2)$  contribution to the interchain exchange.

$$\tilde{J}(\omega, q, \mathbf{q}_\perp) = \hat{Z}^2 \int \frac{d\omega' dq'}{(2\pi)^2} a_\perp^2 \int d^2 k_\perp \left[ \frac{v}{m^2 + \omega'^2 + (vq')^2} \right]^2 T_R \left( \omega' + \frac{\omega}{2}, q' + \frac{q}{2}, \mathbf{k}_\perp \right) \times T_L \left( \omega' - \frac{\omega}{2}, q' - \frac{q}{2}, \mathbf{q}_\perp - \mathbf{k}_\perp \right) . \quad (34)$$

To make the calculations easier, we use the  $k$ -dependence (26) so that the sum over the transverse wave vectors is replaced by integration over  $t$  according to (27). Since  $\tilde{t}(\mathbf{k}_\perp)$  is peaked near zero and  $\mathbf{Q}$ , there are two interesting wave vectors:  $\mathbf{q}_\perp = 0$  and  $\mathbf{q}_\perp = \mathbf{Q}$ .

### A. Case 1: $\mathcal{Z} < \mathcal{Z}_c$

In this case the coherent electron modes still have a gap and no Fermi surface is formed in the RPA. Using (27) to carry out the summation over transverse momenta we obtain

$$\tilde{J}(0, 0, \mathbf{0}) \approx \mathcal{C}_1 \int_0^\infty ds s \frac{\arctan(\mathcal{Z}G(s))}{(1+s^2)^2 G(s)} \equiv \alpha_0 \mathcal{C}_1, \quad (35)$$

where  $\mathcal{Z} = Z_0 t_0 / m$  is defined in (29) and

$$\mathcal{C}_1 = \hat{Z}^2 \kappa_0^2 t_0 \frac{v}{m Z_0} = \frac{\mathcal{Z} \kappa_0^2}{\pi^3 a_0} m, \quad (36)$$

and

$$G(s) = s^{-1} \left[ 1 - \frac{1}{\sqrt{s^2 + 1}} \right]. \quad (37)$$

As expected, this interaction is of order of  $\kappa_0^2 t_0$ . The numerical factor  $\alpha_0$  ranges between 0 for  $\mathcal{Z} = 0$  and 2.81 for  $\mathcal{Z} \rightarrow 3.33019$ . The exchange at momentum transfer  $\mathbf{Q}$  is

$$\begin{aligned} \tilde{J}(0, 0, \mathbf{Q}) &\approx -\frac{\mathcal{C}_1}{2} \int_0^\infty ds s \frac{\ln \left[ \frac{1+\mathcal{Z}G(s)}{1-\mathcal{Z}G(s)} \right]}{(1+s^2)^2 G(s)} \\ &= -\alpha_Q \mathcal{C}_1, \end{aligned} \quad (38)$$

where  $\alpha_Q$  varies between 0 for  $\mathcal{Z} = 0$  and 3.07 for  $\mathcal{Z} \rightarrow \mathcal{Z}_c$ .

### B. Case 2: $\mathcal{Z} > \mathcal{Z}_c$

In this case a Fermi surface in the form of electron and hole pockets is present. The presence of zero energy modes does not really affect the exchange at zero momentum transfer, which is given by

$$\tilde{J}(0, 0, \mathbf{0}) \approx \mathcal{C}_1 \int_0^\infty ds \frac{s f(s)}{(1+s^2)^2 G(s)} = \alpha'_0 \mathcal{C}_1, \quad (39)$$

where

$$\begin{aligned} f(s) &= 2 \arctan(\xi(s) \mathcal{Z} G(s)) - \arctan(\mathcal{Z} G(s)), \\ \xi(s) &= \min(1, [\mathcal{Z} G(s)]^{-1}). \end{aligned} \quad (40)$$

We find that  $\alpha'_0$  starts at 1.405 for  $\mathcal{Z} \rightarrow 3.33019$ , then goes through a maximum of approximately 1.48 around  $\mathcal{Z} \approx 4.18$  and then diminishes slowly. Hence the exchange at wave number zero play a subdominant role.

Let us now turn to the exchange at wavenumber  $\mathbf{Q}$ . We find that there is a logarithmic divergence in (34), which is related to the Fermi surface formation and will be discussed later in more detail. We regularize the divergence by temperature. This may be done by replacing the  $\omega'$ -integral in (34) by a sum over Matsubara frequencies and substituting the finite-temperature Green's function for their  $T = 0$  analogs in the dressed interchain hoppings  $\tilde{T}_{R,L}$  in (34). At low temperatures the single particle Green's function is given by<sup>8</sup>

$$\begin{aligned} G_R(\omega_n, q) &= \int_{-\infty}^\infty dx \frac{A_R(x, q)}{i\omega_n - x}, \\ A_R(\omega, q) &= \frac{Z_0}{4\pi^2 m} \sqrt{\frac{2m}{T}} \left[ \frac{m}{|\omega - vq|} \right]^{\frac{3}{2}} \\ &\times \text{Re} \left[ \sqrt{-2iB} \left( \frac{1}{4} - \frac{i}{2} \frac{\omega^2 - v^2 q^2 - m^2}{2\pi T |\omega - vq|}, \frac{1}{2} \right) \right] \end{aligned} \quad (41)$$

The singular piece of  $\tilde{J}^{\text{sing}}(0, 0, \mathbf{Q})$  diverges logarithmically with temperature and is estimated as

$$\tilde{J}^{\text{sing}}(0, 0, \mathbf{Q}) \approx -\mathcal{C}_1 \ln \left[ \frac{m}{T} \right] \int_{s_-}^{s_+} ds \frac{s [G(s)]^{-1}}{(1+s^2)^2}, \quad (42)$$

where  $s_\pm$  are solutions to the equation

$$1 - \mathcal{Z}G(s_\pm) = 0. \quad (43)$$

In order to establish the exchange at nonzero values of  $\omega$  and  $q$  we have calculated  $\tilde{J}(\omega, q, \mathbf{Q})$  numerically at small temperatures. Rather than using the finite- $T$  Green's function (41) we work with the  $T = 0$  expression (11) and replace  $\omega$  by the discrete Matsubara frequencies. For small temperatures this is a reasonable approximation. We find that  $|\tilde{J}(\omega, q, \mathbf{Q})|$  is largest at  $\omega = 0 = q$ .

In addition to the singular piece (42) there also is a regular contribution to the exchange. As long as we are close to the transition, i.e.

$$\frac{\mathcal{Z} - \mathcal{Z}_c}{\mathcal{Z}_c} \ll 1, \quad (44)$$

we may estimate the regular contribution to the exchange by its value at the critical strength  $\mathcal{Z}_c$  of the interchain tunneling. The latter is given by (38)

$$\tilde{J}^{\text{reg}}(0, 0, \mathbf{Q}) \approx -3.071 \mathcal{C}_1. \quad (45)$$

In the regime (44)

$$\tilde{J}^{\text{sing}}(0, 0, \mathbf{Q}) \approx -1.318 \sqrt{\mathcal{Z} - \mathcal{Z}_c} \mathcal{C}_1 \ln \left[ \frac{m}{T} \right]. \quad (46)$$

The total exchange constant at wave number  $\mathbf{Q}$  is then estimated as

$$\tilde{J}(0, 0, \mathbf{Q}) \approx -\mathcal{C}_1 \left[ 3.071 + 1.318 \sqrt{\mathcal{Z} - \mathcal{Z}_c} \ln \left[ \frac{m}{T} \right] \right] \quad (47)$$

Having determined the exchange constant we are now in a position to estimate the temperature at which a magnetic instability develops. In the absence of interchain

hopping the correlation functions of the matrix field at  $T = 0$  are given by (16). At  $T > 0$  we have

$$\langle g_{\alpha\beta}(\tau, x) g_{\gamma\delta}^+(0, 0) \rangle = \delta_{\alpha\delta} \delta_{\beta\gamma} \frac{\pi T a_0 / v}{2 \left| \sinh \left( \frac{\pi T}{v} [x + iv\tau] \right) \right|}, \quad (48)$$

if we neglect the marginally irrelevant current-current interaction in the spin-sector of the Hamiltonian (9) describing the 1D Mott insulating chains. If one takes it into account in renormalization group improved perturbation theory one obtains<sup>16</sup>

$$\langle \text{tr}(g\sigma^\alpha) \text{tr}(g^\dagger \sigma^\beta) \rangle = \delta_{\alpha\beta} \frac{\sqrt{\ln \left[ \frac{\Lambda}{T} \right]} \pi T a_0 v^{-1}}{\left| \sinh \left( \frac{\pi T}{v} [x + iv\tau] \right) \right|}, \quad (49)$$

where  $\Lambda$  is a high-energy cutoff, which we may take to be of the order of the hopping integral along the chain direction. Carrying out an analogous calculation for the dimerization operator we find

$$\langle \text{tr}(g) \text{tr}(g^\dagger) \rangle = \delta_{\alpha\beta} \frac{\left[ \ln \left[ \frac{\Lambda}{T} \right] \right]^{-\frac{3}{2}} \pi T a_0 v^{-1}}{\left| \sinh \left( \frac{\pi T}{v} [x + iv\tau] \right) \right|}. \quad (50)$$

Upon Fourier transformation and analytical continuation one finds the following result for the dynamical magnetic susceptibility of the uncoupled chain system<sup>17</sup>

$$\chi_{1d}(\omega, q) = -\frac{a_0 \sqrt{\ln \left[ \frac{\Lambda}{T} \right]} \Gamma \left[ \frac{1}{4} - i \frac{\omega - vq}{4\pi T} \right] \Gamma \left[ \frac{1}{4} - i \frac{\omega + vq}{4\pi T} \right]}{2T \Gamma \left[ \frac{3}{4} - i \frac{\omega - vq}{4\pi T} \right] \Gamma \left[ \frac{3}{4} - i \frac{\omega + vq}{4\pi T} \right]}. \quad (51)$$

The dimerization susceptibility is equal to (51) apart from the prefactor, in which  $\sqrt{\ln[\Lambda/T]}$  is replaced by  $[\ln[\Lambda/T]]^{-3/2}$ . Hence the staggered spin susceptibility is always more singular than the dimerization susceptibility and as a result the dominant instability of the spin sector is towards Néel order. The enhancement of the spin susceptibility as compared to the dimerization susceptibility is caused by the leading irrelevant operator in the Hamiltonian, namely the interaction of spin currents. If we were to add an interaction to the underlying lattice Hamiltonian in order to eliminate this interaction, the symmetry between dimerization and the staggered components of the spins would be broken by some other irrelevant operator. The dynamical susceptibility of the coupled chains system can be determined by an expansion in the interchain coupling of the type discussed in<sup>12,13</sup>. The leading term is given by the Random Phase Approximation

$$\chi_{3d}(\omega, q, \mathbf{p}_\perp) = \frac{\chi_{1d}(\omega, q)}{1 - 2\tilde{J}(\omega, q, \mathbf{p}_\perp) \chi_{1d}(\omega, q)}. \quad (52)$$

Given the expression (52) for the dynamical susceptibility we may obtain an estimate for the transition temperature  $T_c$  below which three dimensional magnetic long range order develops.  $T_c$  is defined as the temperature at

which a zero frequency pole develops in  $\chi_{3d}$ . Given that  $\chi_{1d}(0, q)$  is peaked at  $q = 0$  and  $\tilde{J}$  is peaked at  $q = 0$  and  $\mathbf{p} = \mathbf{Q}$  we obtain the following condition fixing  $T_c$

$$1 - 2\tilde{J}(0, 0, \mathbf{Q}) \chi_{1d}(0, 0) = 0. \quad (53)$$

Replacing  $\tilde{J}(0, 0, \mathbf{Q})$  by (47) we arrive at the following equation determining the transition temperature  $T_c$

$$\begin{aligned} \frac{T_c}{m} \approx & 2.887 \kappa_0^2 \sqrt{\ln \left[ \frac{\Lambda}{T_c} \right]} \\ & \times \left[ 1 + 0.429 \sqrt{\mathcal{Z} - \mathcal{Z}_c} \ln \left[ \frac{m}{T_c} \right] \right]. \end{aligned} \quad (54)$$

Let us consider the two limiting cases in which either the regular (45) or the singular part (46) of the exchange dominates and drives the transition. The first case occurs if we are very close to the point where the Fermi pockets are first formed and  $\mathcal{Z} - \mathcal{Z}_c \ll (\ln(\kappa_0^2))^{-2}$ . Then the transition temperature is roughly equal to

$$\frac{T_c}{m} \approx 2.887 \kappa_0^2 \sqrt{\ln \left[ \frac{\Lambda}{m \kappa_0^2} \right]}. \quad (55)$$

The second case occurs if  $\mathcal{Z} - \mathcal{Z}_c \gg (\ln(\kappa_0^2))^{-2}$  and then

$$\frac{T_c}{m} \approx 1.239 \kappa_0^2 \delta \sqrt{\ln \left[ \frac{\Lambda}{m \kappa_0^2 \delta} \right] \ln \left[ \frac{1}{\kappa_0^2 \delta} \right]}, \quad (56)$$

where  $\delta = \sqrt{\mathcal{Z} - \mathcal{Z}_c}$ .

## V. EFFECTIVE THEORY AT LOW ENERGIES; THE RESIDUAL INTERACTIONS

Now we are in position of writing the low-energy effective action for the metallic state. This effective action describes interactions of the low-energy modes i.e. the coherent fermions and the order parameter field  $g_{ab}$ . In the previous section we calculated the interchain coupling for the  $g$ -field. It contains a part coming from states far from the chemical potential and the part with logarithmic divergences coming from the states close to the Fermi surface. We can isolate the first piece and include it into the effective action of  $g$

$$\begin{aligned} S_{\text{sp}} = & \sum_{\mathbf{n}} W[g_{\mathbf{n}}] \\ & + \sum_{\mathbf{m}, \mathbf{l}} J_{\mathbf{ml}} \int d\tau dx \text{Tr} \left[ g_{\mathbf{m}}(\tau, \mathbf{x}) g_{\mathbf{l}}^\dagger(\tau, \mathbf{x}) \right], \end{aligned} \quad (57)$$

where to first approximation

$$J_{\mathbf{nl}} \approx \frac{Z_0^2}{\pi^2 m a_0} t_{\mathbf{nl}}^2. \quad (58)$$

This part of the action plays the role of the sigma model in the spin-fermion model by Pines and Chubukov (see<sup>2</sup>



and references therein). Taken in isolation, this model has an instability at some temperature  $T_c$  which can be estimated from the RPA expression for the dynamical magnetic susceptibility in complete analogy with our calculation in section IV B. Since the coherent fermions are low-energy excitations, they cannot be simply integrated out, but their interaction with  $g$ -field should be added to the action. The Fermi surface of the coherent fermions is determined by the equation

$$G_0(0, q) \tilde{t}_\perp(\mathbf{k}_\perp) = 1, \quad (59)$$

and consists of four pockets (two electron-like ones and two hole-like ones) as is shown in Fig.3. Let us consider the situation where the scale of the interchain hopping  $t_0$  is very slightly larger than the minimal value  $\bar{t}_0$  required for the formation of a Fermi surface

$$t_0 = \bar{t}_0 + \delta t = \sqrt{\frac{11 + 5\sqrt{5}}{2}} \frac{m}{Z_0} + \delta t. \quad (60)$$

The electron and hole pockets are then shallow and anisotropic and the Fermi surface is determined by the equation

$$E(q, \mathbf{k}_\perp) = 0, \quad (61)$$

where

$$E(q, \mathbf{k}_\perp) = A_\parallel m \frac{(q - q_0)^2}{q_0^2} + A_\perp m \frac{|\mathbf{k}_\perp a_\perp|^2}{\kappa_0^2} - E_0, \quad (62)$$

$$E_0 \approx 0.352\delta t, \quad \frac{vq_0}{m} = \left[ \frac{1 + \sqrt{5}}{2} \right]^{\frac{1}{2}} \approx 1.27202,$$

$$A_\parallel \approx 0.543, \quad A_\perp \approx 1.27202. \quad (63)$$

The electron pockets are formed at  $(k_F + q, \mathbf{k}_\perp)$  and  $(-k_F - q, \mathbf{k}_\perp)$  whereas the hole pockets are located at  $(k_F - q, \mathbf{Q} + \mathbf{k}_\perp)$  and  $(-k_F + q, \mathbf{Q} + \mathbf{k}_\perp)$ , where  $q$  and  $\mathbf{k}_\perp$  are determined from (61). Let us denote the annihilation

operator of the coherent fermions by  $\Psi(\tau, q, \mathbf{k}_\perp)$ . The soft modes occur in the vicinity of the electron and hole pockets and it is convenient to decompose  $\Psi(\tau, q, \mathbf{k}_\perp)$  accordingly. We denote by  $R_e(\tau, q, \mathbf{p}_\perp)$  and  $L_e(\tau, q, \mathbf{p}_\perp)$  the annihilation operator in the vicinity of the electron pockets and  $(q, \mathbf{p}_\perp)$  is the deviation from  $(\pm k_F, \mathbf{0})$ . Similarly we denote by  $R_h(\tau, q, \mathbf{p}_\perp)$  and  $L_h(\tau, q, \mathbf{p}_\perp)$  the annihilation operator in the vicinity of the hole pockets and  $(q, \mathbf{p}_\perp)$  is the deviation from  $(\pm k_F, \mathbf{Q})$ .

From Eq.(62) we determine the particle density associated with a single pocket is

$$n \approx 0.027 a_\perp^{-2} q_0 \kappa_0^2 (\mathcal{Z} - \mathcal{Z}_c)^{3/2} \quad (64)$$

The liquid of quasi-particles becomes degenerate at temperatures of order of  $E_0$ . Comparing it with the transition temperatures (54), (56) we conclude that the degenerate metallic state exists only at

$$\mathcal{Z} - \mathcal{Z}_c \gg \kappa_0^2. \quad (65)$$

corresponding to  $na_\perp^2 \gg 0.027 q_0 \kappa_0^5$ . Close to the Fermi surface the Green's function (28) can be approximated as

$$G(\omega, \pm k_F + q, \mathbf{k}_\perp) \approx \frac{Z_2}{i\omega - E(\pm q, \mathbf{k}_\perp)}, \quad (66)$$

$$G(\omega, \pm k_F + q, \mathbf{k}_\perp + \mathbf{Q}) \approx \frac{Z_2}{i\omega + E(\mp q, \mathbf{k}_\perp)}, \quad (67)$$

where

$$Z_2 \approx \frac{vq_0}{\bar{t}_0} \approx 0.352. \quad (68)$$

The expressions (67) exhibit the particle-hole symmetry characteristic of our model at half-filling. As usual, we include the residue  $Z$  in the coupling constant and replace the fermionic action by the action of four components of free fermions. The effective action describing the fermions is then given by

---


$$S_f = a_\perp^2 \int \frac{d\tau d^3\mathbf{k}}{(2\pi)^3} [R_{a,\alpha}^*(\tau, \mathbf{k}) (\partial_\tau - E_a^R(\mathbf{k})) R_{a,\alpha}(\tau, \mathbf{k}) + L_{a,\alpha}^*(\tau, \mathbf{k}) (\partial_\tau - E_a^L(\mathbf{k})) L_{a,\alpha}(\tau, \mathbf{k})], \quad (69)$$


---

where  $\mathbf{k} = (q, \mathbf{k}_\perp)$ ,  $\alpha = \uparrow, \downarrow$ ,  $a = e, h$  and

$$E_e^{R,L}(\mathbf{k}) = E(\pm q, \mathbf{k}_\perp), \quad E_h^{R,L}(\mathbf{k}) = -E(\mp q, \mathbf{k}_\perp). \quad (70)$$

The fermion-spin vertex is described by the action

$$S_{\text{int}} = a_\perp^4 \int \frac{d\tau d^3\mathbf{k} d^3\mathbf{k}'}{(2\pi)^6} \mathcal{L}_{\text{int}}, \quad (71)$$

where

$$\begin{aligned} \mathcal{L}_{\text{int}} = & I_{\mathbf{k},\mathbf{k}'} \sum_{a=e,h} R_{a,\alpha}^*(\tau, \mathbf{k}) L_{a,\beta}(\tau, \mathbf{k}') g_{\alpha\beta}(\tau, \mathbf{k} - \mathbf{k}') \\ & + I_{\mathbf{k},\mathbf{Q}+\mathbf{k}'} R_{e,\alpha}^*(\tau, \mathbf{k}) L_{h,\beta}(\tau, \mathbf{k}') g_{\alpha\beta}(\tau, \mathbf{k} - \mathbf{Q} - \mathbf{k}') \\ & + I_{\mathbf{Q}+\mathbf{k},\mathbf{k}'} R_{h,\alpha}^*(\tau, \mathbf{k}) L_{e,\beta}(\tau, \mathbf{k}') g_{\alpha\beta}(\tau, \mathbf{k} + \mathbf{Q} - \mathbf{k}') \\ & + \text{h.c.}, \\ I_{\mathbf{k},\mathbf{k}'} = & 2\pi \frac{v\hat{Z}Z_2}{m^2} \tilde{t}_\perp(\mathbf{k}) \tilde{t}_\perp(\mathbf{k}'). \end{aligned} \quad (72)$$

All wave vectors in the above formulae lie close to the non-interacting Fermi surface and therefore their longitudinal components are small in comparison to  $\pi$ :  $|q| \ll \pi a_0$ . The entire approach is valid only when the volume inside of the Fermi surfaces is small. One then can neglect the momentum dependence of the exchange constant in Eq.(72). The sign of the exchange constant depends on

the “pocket index”  $a, b$

$$I_{ab} \approx \gamma m \begin{pmatrix} 1 & -1 \\ -1 & 1 \end{pmatrix}, \quad (73)$$

where  $\gamma$  is a constant. The interaction can be cast in the form

$$\mathcal{L}_{int} = \gamma m \left[ \sum_a R_{a,\alpha}^*(\mathbf{k}) L_{a,\beta}(\mathbf{k}') g_{\alpha\beta}(\mathbf{k} - \mathbf{k}') - \left\{ R_{e,\alpha}^*(\mathbf{k}) L_{h,\beta}(\mathbf{k}') + R_{h,\alpha}^*(\mathbf{k}) L_{e,\beta}(\mathbf{k}') \right\} g_{\alpha\beta}(\mathbf{k} - \mathbf{k}' - \mathbf{Q}) \right] + \text{h.c.} \quad (74)$$

The value of the coupling constant  $\gamma$  can be extracted from Eqns (42) and (76) by noting that it is this interaction which gives rise to the logarithmic singularity in  $J(Q)$

$$\tilde{J}^{\text{sing}}(0, 0, \mathbf{Q}) \approx -2\gamma^2 m^2 \frac{\rho(0)}{a_0} \ln \left[ \frac{\delta t}{T} \right]. \quad (75)$$

Here  $\rho(0)$  is the density of states per species at the Fermi surface of coherent fermions

$$\begin{aligned} \rho(0) &= \lim_{\omega \rightarrow 0} a_0 \int \frac{d^3 \mathbf{k}}{(2\pi)^3} \left[ -\frac{1}{\pi} \text{Im} G(\omega, k_F + q, \mathbf{k}_\perp) \right] \\ &\approx 0.539 \frac{a_0}{(2\pi)^2} \frac{\kappa_0^2}{v} \left[ \frac{\delta t}{t_0} \right]^{\frac{1}{2}}. \end{aligned} \quad (76)$$

The result is that close to the transition we have

$$\gamma \propto \sqrt{\frac{t}{m}}, \quad (77)$$

where  $t \gg m$  is the hopping along the chains and the constant of proportionality is of order 1. Though  $\gamma$  is never small, the small parameter  $\kappa_0^2$  appears every time one integrates over the transverse momentum. Hence the magnitude of  $\gamma$  is not a problem. The effective action describing the metallic side of the Mott-insulator to metal transition is given by Eqns (57), (69) and (74). We find it instructive to write it down also in position space

$$\begin{aligned} S_f &= \int d\tau d^3 \mathbf{x} \Psi_\alpha^\dagger(\tau, \mathbf{x}) \left\{ (I \otimes I) \partial_\tau + (I \otimes \tau^z) \left[ E_0 + \frac{\partial_x^2}{2M_\parallel} + \frac{\vec{\nabla}_\perp^2}{2M_\perp} \right] \right\} \Psi_\beta(\tau, \mathbf{x}), \\ S_{int} &= \frac{\gamma m}{2} \int d\tau d^3 \mathbf{x} \Psi_\alpha^\dagger(\tau, \mathbf{x}) \left( \{ \tau^+ \otimes [\exp(-2iq_0 x \tau^z) - \tau^x \exp(-i\mathbf{Q} \cdot \mathbf{x}_\perp)] \} g_{\alpha\beta}(\tau, \mathbf{x}) + \text{h.c.} \right) \Psi_\beta(\tau, \mathbf{x}). \end{aligned} \quad (78)$$

Here we have taken the continuum limit in the directions perpendicular to the chains and introduced a field  $\Psi_\alpha^+ = (\phi^* R_{e,\alpha}^+, \phi R_{h,\alpha}^+, \phi L_{e,\alpha}^+, \phi^* L_{h,\alpha}^+)$ , where  $\phi = \exp(iq_0 x)$ . We employ a tensor-product notation, where the first space is associated with the “right/left” index and the second space with the “e/h” index. The Fermi surfaces of electrons and holes are shifted to the origin and superimposed. The spin action  $S[g]$  is given by Eq.(57). Alternatively, one may use the Abelian representation given by Eq.(9), with  $g$  defined by (15).

### A. Marginal Fermi liquid

As we shall now demonstrate, at temperatures higher than the Néel temperature  $T_c$  this metal is, in fact

a Marginal Fermi Liquid<sup>19</sup>. The following discussion closely parallels the analysis given by Chubukov *et al* for the spin-fermion model (see, for example Ref.[2]). Let us consider diagrams for the Green’s function of right moving electrons. We expand around uncoupled chains and take both the spin-fermion coupling and interchain spin-spin exchange into account perturbatively. The elements of the diagram technique for the fermionic degrees of freedom are as usual, whereas the building blocks in the spin sector are the connected 2n-point spin correlators for a single chain. In diagrams that do not contain closed fermionic loops or the interchain exchange such as the ones in Figs 7a and 7b, the spin correlations are independent of the transverse wave vector. This means that each fermion Green’s function is integrated over  $k_\perp$ . This integral does not differ significantly from the inte-

gral over all momenta and as a result is independent of  $q_{\parallel}$ , corresponding to a Green's function that is local in real space:

$$\int \frac{d\mathbf{k}_{\perp}^2}{(2\pi)^2} \frac{1}{i\omega - E_e^L(q, \mathbf{k}_{\perp})} \approx \text{const } i\kappa_0^2 \text{sgn}(\omega). \quad (79)$$

As (79) is independent of  $q$ , we may integrate the spin correlator in the diagram of Fig. 7a over  $q$ . This makes the spin correlator local. As a result the contributions to the self energy which do not contain closed fermionic loops or interchain spin exchange are approximately momentum independent. Then the self energy calculation becomes essentially a local problem like the problem of electron-phonon interactions in metals and superconductors (the Eliashberg theory)<sup>18</sup>. In fact, such an approach works under less stringent conditions, namely, when the spin excitations in the transverse direction are much slower than the quasi-particles. Therefore the diagrams generating a  $\mathbf{k}_{\perp}$  dependence of the spin-spin correlators, such as the ones in Fig. 7c) and Fig. 7d) do not affect the result for the electron self energy even close to the transition. Once such diagrams are neglected, we get an expansion where a factor  $\kappa_0^2$  is associated with each fermionic line (originating from the integration over  $\mathbf{k}_{\perp}$ , as in Eq.(79). Since  $\Sigma$  depends only on frequency, making these lines fat does not change the result (79) and no self-consistency is required. The contribution from the

The contribution of the diagram in Fig. 7a) to the self-energy is then

$$\begin{aligned} \Sigma^{(a)}(\omega) &\propto \kappa_0^2 \left( \ln \left[ \frac{\Lambda}{T} \right] \right)^{\frac{1}{2}} \int d\tau \frac{e^{i\omega\tau} T}{\tau |\sin(\pi T\tau)|} \\ &\sim i\kappa_0^2 \omega \ln \left[ \frac{E_0}{\max\{\omega, T\}} \right] \left( \ln \left[ \frac{\Lambda}{T} \right] \right)^{\frac{1}{2}}. \end{aligned} \quad (81)$$

Here  $E_0^{-1}$  serves as a short-time cutoff in all integrals. The diagram in Fig 7b) involves cumulants of the type

$$\langle\langle e^{\frac{i}{2}\Theta(\tau_1)} e^{-\frac{i}{2}\Theta(\tau_2)} e^{\frac{i}{2}\Theta(\tau_3)} e^{-\frac{i}{2}\Theta(\tau_4)} \rangle\rangle \quad (82)$$

and gives a contribution

$$\begin{aligned} \Sigma^{(b)}(\omega) &\propto \kappa_0^6 \int d\tau_2 d\tau_3 d\tau_4 \frac{e^{i\omega\tau_{14}}}{\tau_{12}\tau_{23}\tau_{34}} \\ &\times \left[ \left| \frac{\tau_{13}\tau_{24}}{\tau_{12}\tau_{14}\tau_{23}\tau_{34}} \right| - \frac{1}{|\tau_{12}\tau_{34}|} - \frac{1}{|\tau_{14}\tau_{23}|} \right] \propto \omega^2 \end{aligned} \quad (83)$$

to the self energy. Various other contributions are zero because some local cumulants vanish

$$\langle\langle e^{\frac{i}{2}\Phi(\tau_1)} e^{-\frac{i}{2}\Theta(\tau_2)} e^{\frac{i}{2}\Theta(\tau_3)} e^{-\frac{i}{2}\Phi(\tau_4)} \rangle\rangle = 0. \quad (84)$$

Equation 4point shows that contributions from higher cumulants can be neglected at small frequencies. As a result, the only essential contribution to the self energy comes from the diagram Fig. 7a and is given by Eq. (81).

## VI. THE ORDERED STATE

As we have discussed in the previous sections, the system undergoes an antiferromagnetic transition at a temperature much smaller than the Mott-Hubbard gap  $T_c \sim m\kappa_0^2$ . Once  $T_c$  becomes small compared to the quasi-particle Fermi energy  $E_0$ , one can distinguish between metallic and insulating behavior. As we have demonstrated, the corresponding metal is rather unusual, being in fact a Marginal Fermi Liquid. Below  $T_c$  however, the system becomes either an insulator (for zero doping) or an ordinary Fermi liquid. Indeed, at zero doping the electron and hole Fermi surfaces are nested and the ordering occurs at the antiferromagnetic wave vector in the transverse direction (recall that the chains run along the  $z$ -axis) such that

$$\langle g_{l,\alpha\beta}(x) \rangle = \vec{\sigma}_{\alpha\beta} \cdot \mathbf{M} (-1)^{l_x + l_y}. \quad (85)$$

Here the components of  $\vec{\sigma}$  are the Pauli matrices and  $\mathbf{M}$  is the ordering vector. In the mean-field approximation the fermionic spectrum is gapped

$$\omega_a^2 = (E_a^R(\mathbf{k}))^2 + \gamma^2 m^2 |\mathbf{M}|^2, \quad a = e, h. \quad (86)$$

At non-zero doping our approach still holds provided the chemical potential lies inside the Mott-Hubbard gap. There is no nesting any longer and the magnetic ordering does not open a gap in the quasi-particle spectrum. As usual, magnetic fluctuations interact with quasi-particles through gradient vertices and these interactions are weak.

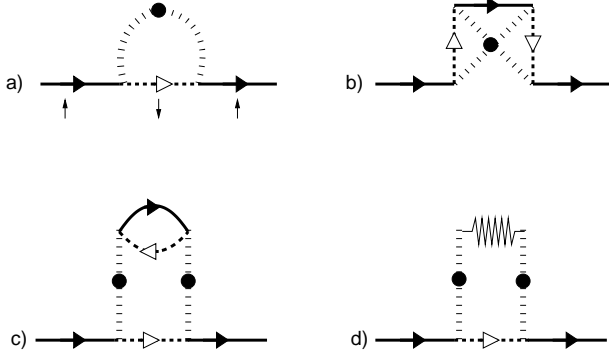


FIG. 7: Diagrams for the quasi-particle self energy of right-moving electrons. The lines with arrows represent the fermionic Green's functions of right and left moving electrons and holes. The 2n-point vertices denote cumulants of the matrix fields  $g$  and  $g^\dagger$ .

diagram Fig. 7a contains the correlation function

$$\langle\langle e^{\frac{i}{2}\Theta(\tau_1)} e^{-\frac{i}{2}\Theta(\tau_2)} \rangle\rangle \simeq \frac{\left( \ln \left[ \frac{\Lambda}{T} \right] \right)^{1/2} \pi T v^{-1}}{|\sin(\pi T[\tau_1 - \tau_2])|}. \quad (80)$$

## VII. CONCLUSIONS

The main result of this paper is a formulation of a self-consistent description of the hybrid state of 3D quasi-particles interacting with magnetic collective modes. The derivation is done for a toy model of half filled Hubbard chains weakly coupled through a long range inter-chain hopping. A certain artificiality of the model was necessary to ensure the self-consistency of our approach through the presence of a small parameter  $\kappa_0^2$ . We have also neglected the long-range component of the Coulomb interaction, which plays an important role in determining the character of the metal-insulator transition. In reality a long-range interaction may lead to an instability of the small FS phase, though for small Mott-Hubbard gap its influence is diminished by the presence of a large dielectric constant. In this case the first order MI transition line may terminate below the antiferromagnetic transition line of Fig. 1.

The resulting low energy effective theory is of the Eliashberg type: the interaction between quasi-particles and collective modes leads to strong retardation effects resulting in a strongly frequency dependent quasi-particle self energy. In the present model this takes place not just at the 'hot spots', as in the spin-fermion model of Chubukov and Pines, but on the entire quasi-particle FS. This makes the present model a candidate for the description of 'bad' metals. The fact that in our model the electron self energy is of the Marginal Fermi Liquid form

is not universal and is determined by the particular spin fluctuation spectrum.

As we discussed in the introduction, our theory provides an example of a state where the number of carriers is unrelated to the volume of the FS. Though this idea is well established (see e.g. the textbook [5]), its microscopic realization was restricted to superconductors (the example given in Ref.[5]). Our model provides another example. It also demonstrates that one does not need exotic ground states to have a small FS, as was suggested in Refs [20], [21]. The small FS phenomenology can be generalized beyond our model. In general there is no *a priori* reason for the Fermi surface even to be closed; for instance, Ref.[22] describes a state with a truncated Fermi surface observed in ARPES experiments on undoped cuprates<sup>9</sup>.

## Acknowledgments

We are grateful to Andrei Chubukov for numerous discussions and interest to the work. AMT is grateful to S. Buehler-Paschen for information about Hall effect measurements. AMT acknowledges support by the US Department of Energy under contract number DE-AC02-98 CH 10886. FHLE is supported by the EPSRC under grant GR/R83712/01 and the Institute for Strongly Correlated and Complex Systems at BNL.

- 
- <sup>1</sup> D. Pines, Z. Phys. **B103**, 129 (1997).
  - <sup>2</sup> A. Abanov, A.V. Chubukov and J. Schmalian, Adv. Phys. **52**, 119 (2003); A. V. Chubukov, D. Pines and J. Schmalian, cond-mat/0201140.
  - <sup>3</sup> F. H. L. Essler and A. M. Tsvelik, Phys. Rev **B65**, 115117 (2002).
  - <sup>4</sup> J.M. Luttinger, Phys. Rev. **119**, 1153 (1960).
  - <sup>5</sup> A.A. Abrikosov, L.P. Gorkov and I.E. Dzyaloshinski, *Methods of Quantum Field Theory in Statistical Physics*, Dover (New York) 1975, page 168.
  - <sup>6</sup> I.E. Dzyaloshinski, Phys. Rev. **B68**, 085113 (2003).
  - <sup>7</sup> B. L. Altshuler, A. V. Chubukov, A. Dashevskii, A. M. Finkel'stein, D. K. Morr, Europhys. Lett. **41**, 401 (1998).
  - <sup>8</sup> F. H. L. Essler and A. M. Tsvelik, Phys. Rev. Lett. **90**, 126401 (2003).
  - <sup>9</sup> M. R. Norman *et al.*, Nature (London), **392**, 157 (1998).
  - <sup>10</sup> S. Buehler-Paschen *et al.*, submitted to Nature.
  - <sup>11</sup> D. Boies, C. Bourbonnais and A.-M.S. Tremblay, Phys. Rev. Lett. **74**, 968 (1995).
  - <sup>12</sup> M. Bocquet, F.H.L. Essler, A.M. Tsvelik and A. Gogolin, Phys. Rev. **B64**, 094425 (2001); M. Bocquet, Phys. Rev. **B65**, 184415 (2002).
  - <sup>13</sup> V.Y. Irkhin and A.A. Katanin, Phys. Rev. **B61**, 6757 (2000).
  - <sup>14</sup> S. Lukyanov and A. B. Zamolodchikov, Nucl. Phys. **B607**, 437 (2001).
  - <sup>15</sup> M. Dzero and L. P. Gor'kov, Phys. Rev. **B69**, 092501 (2004).
  - <sup>16</sup> V. Barzykin, J. Phys. Cond. Mat. **12**, 2053 (2000).
  - <sup>17</sup> H. J. Schulz and C. Bourbonnais, Phys. Rev. **B27**, 5856 (1983).
  - <sup>18</sup> G. M. Eliashberg, Sov. Phys. JETP **11**, 696 (1960); D. J. Scalapino in *Superconductivity*, Vol. 1, p. 449, ed. by D. Parks, Dekker Inc. N.Y. 1969; F. Marsiglio and J. P. Carbotte, in *The Physics of Conventional and Unconventional Superconductors*, ed. by K. H. Bennemann and J. B. Ketterson, Springer-Verlag.
  - <sup>19</sup> C. M. Varma, P. B. Littlewood, S. Schmitt-Rink, E. Abrahams, and A. E. Ruckenstein, Phys. Rev. Lett. **63**, 1996 (1989).
  - <sup>20</sup> T. Senthil, S. Sachdev and M. Vojta, Phys. Rev. Lett. **90**, 216403 (2003).
  - <sup>21</sup> T. Senthil, M. Vojta and S. Sachdev, Phys. Rev. **B69**, 035111 (2004).
  - <sup>22</sup> C. Honerkamp, M. Salmhofer, N. Furukawa and T. M. Rice, Phys. Rev. **B63**, 035109 (2001).